Institut für Numerische Simulation
Rheinische Friedrich-Wilhelms-Universität Bonn

Wegelerstraße 6 • 53115 Bonn • Germany
phone +49 228 73-3427 • fax +49 228 73-7527
www.ins.uni-bonn.de

H. Manzano, J.S. Dolado, M. Griebel, and J. Hamaekers

A molecular dynamics study of the aluminosilicate chains structure in Al-rich calcium silicate hydrated (C-S-H) gels

INS Preprint No. 0707

November 2007

A molecular dynamics study of the aluminosilicate chains structure in Al-rich calcium silicate hydrated (C-S-H) gels.

H. Manzano[*,1], J.S. Dolado[1,2], M. Griebel[3], and J. Hamaekers[3].

[1] LABEIN-Tecnalia, Parque Tecnológico de Bizkaia, Derio, Spain.
[2] Nanostructured and Eco-efficient Materials for Construction Unit, Associated Unit LABEIN-Tecnalia/CSIC, Spain.
[3] Institute for Numerical Simulation, University of Bonn, Germany.

Calcium silicate hydrated (C-S-H) gel is the principal binding phase of the cement paste and responsible for its strength. It is basically composed of silicate chains held together with CaO layers, where different guest ions can enter its structure. In particular, the substitution of Al in the silicate chains is expected to play a decisive role for the resulting properties of the cementitious materials. This work explores by means of molecular dynamics simulation the incorporation of aluminium into C-S-H gel. For that purpose we simulate the polymerisation of C-S-H gel in presence of Al atoms and analyse both the connectivity of the (alumino)silicate chains and the position of the aluminium atoms within the structure of C-S-H gel.

1. Introduction

C-S-H gel is the most important component of any cement paste, because it is primarily responsible for the cohesion and hardness of the material.[1] It is an X-ray amorphous product with variable composition, usually characterized by its Ca/Si ratio. Several models [1-3] depict C-S-H gel as silicate chains held together with calcium oxide sheets, forming layered structures (see Figure 1). These structures have resemblances with a natural crystalline family, called tobermorite. Most of the knowledge of the atomic structure of the C-S-H gel has been gained by comparison with these ordered structures.

Among all experimental techniques employed in the characterization of the C-S-H gel [4], NMR is probably the one which supplies most information about the silicate chain structure in C-S-H gel so far [5]. The chains follow a wollastonite-like or *dreierketten* arrangement, in which the smallest repeat unit contains three silicate tetrahedrons. As consequence, two different sites appear in the chains, pairing sites and bridging sites [1-3]. The chain length is determined by the 3n-1 rule, n being an integer, which gives rise to discrete values of silicate tetrahedron units of 2, 5, 8, etc. There is generally a prevalence of dimeric structures, although longer chains are formed for low Ca/Si ratios as well [6-8]. The natural crystalline species of the tobermorite family follow this structure, with the exception that the silicate chains are infinite [9, 10].

Among the possible guest-ions which can be accommodated in the C-S-H gel, aluminium is the most

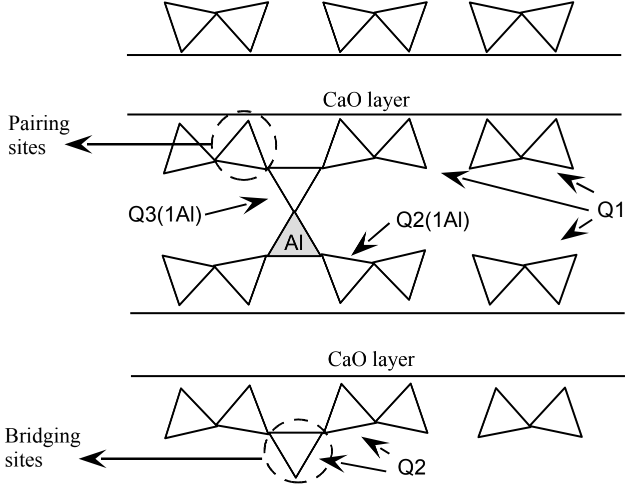

Figure 1. Schematic representation of the structure of C-S-H gel. Each triangle represents the tetrahedral configuration of a SiO$_4^{-4}$ unit (an AlO$_4^{-5}$ unit is marked). Pairing and bridging sites are shown. The Qn notation for some units is also given, see section 3 for more details.

---

[1] In cement chemistry notation C represents calcium oxide (CaO), S silicon oxide (SiO$_2$) and H water. C-S-H implies a variable composition of these species.

---

[*] Corresponding author: hmanzano@labein.es.

common one. Several authors have investigated its incorporation by means of ^{27}Al and ^{29}Si NMR. It is the common understanding in the literature that Al substitutes for Si in the tetrahedral chain, and that there is no significant substitution for Ca in the oxide layers [11-15]. Within the chains, the incorporation of aluminium is also restricted to certain sites. According to most of the authors, the substitution of Al for Si does not occur in terminating positions of the chains, but mainly at the bridging sites (BS) of the silicate chains [11-16]. However, Faucon et al. [17] reported that the incorporation of aluminium takes place in different positions depending on the Al/Si and Ca/Si ratios. They suggest that for low Al/(Si+Al) ratios the aluminium ions are located in the Q2 pairing sites (PS) of the silicate chains. When the Al content and the Ca/Si ratio rise, there happens a reorganization of the chains and the Al atoms migrate to the bridging sites. They concluded that the substitution in Q2 non-bridging sites is possible, although it is not stable. The incorporation of Al in the silicate chains is experimentally known to increase the silicate main chain length (MCL) of C-S-H gels when compared with Al-free samples [11-15]. Assuming the tobermorite-like model [1-3], the C-S-H gel with aluminium is likely to be composed mainly of pentamers, with a certain portion of dimers and a lower amount of longer structures as octamers [11]. For pastes with low Ca/Si ratios, it has been found that not only longer chains are formed, but also non-linear structures are created [15]. The appearance of Q3 units implies the formation of branches along the linear chains. If the tobermorite-like model is assumed, these branches mean the establishment of linkages between different chains at the bridging sites. It is worth noting that Q3 peaks also appear in Al-free C-S-H gel at low Ca/Si rations [18, 29], but aluminium atoms exhibit a clear ability for occupying these sites [15].

Some works have explored the aluminium substitution from a computational point of view. Faucon et al. [19] concluded from a molecular dynamics simulation of Hamid´s tobermorite with Al substituted [20] that the infinite chain structure of the crystal breaks when Al substitutes for Si in the pairing sites (PS), whereas it is kept unchanged if the substitution takes place in the bridging positions (BS). Yamanaka et al. performed semi-empirical and ab initio calculations with non conclusive results, and found different stable positions depending on the employed method [21]. Finally, Nagasaka et al. suggested from the results of their ab initio simulations [22] that, in isolated silicate chains at thermodynamic equilibrium, the substitution of Al for Si is possible in all positions.

In this work we apply the molecular dynamics method to study the position of Al in the silicate chains, as well as the involved changes in the chain structure. Our calculations, unlike the previous ones, do not take as starting point a pre-fixed structure related to C-S-H gel, but simulate the formation of the chains in a polymerisation process. The results are compared with experimental studies and previous simulations of Al-free C-S-H gels [23].

2. Computational procedure

We apply the molecular dynamics approach to study the polymerisation of Si(OH)$_4$ and Al(OH)$_3$ in presence of Ca(OH)$_2$ · 4 H$_2$O and Na(OH) · 5 H$_2$O (which plays the role of a counter-ion balancing the charge excess of Al^{+3} for Si^{+4} substitution [14, 16]). To this end, we follow the procedure to simulate Al-free C-S-H gels employed in Ref. [23]. The Si, O, and H interactions are modelled by the Feuston-Garofalini [24] potential energy function in the variant of Lintton and Garofalini [25], which is especially suitable to describe condensation reactions. For the Si, O, Ca, and Al interactions we apply a further variant given by Zhang and Garofalini [26] and for the interactions of Na with Si, O, and Al we employ the variant given by Webb and Garofalini [27]. Analogously to Ref. [23] we additionally apply a screened Coulomb potential term $q_iq_jerfc(r_{ij}/\beta_{ij})/r_{ij}$ to describe the remaining repulsive interactions for the atom pairs Ca-Na, Ca-H, and Na-H. Here, q_i denotes the ionic charge of particle i, r_{ij} denotes the distance between particle i and particle j, β_{ij} is an interaction-dependent parameter, and *erfc* stands for the complementary error function. We set the parameters to $\beta_{Ca\text{-}Na}=2.3$ Å and $\beta_{Ca\text{-}H}=\beta_{Na\text{-}H}=2.31$ Å and use $q_{Ca}=+2$ and $q_{Na}=q_H=+1$ for the ionic charges.

To perform molecular dynamics simulations in the canonical ensemble (NTV) we use the so-called Nosé Langrangian [28], where we employ a predictor-corrector scheme based on the approach of Beeman and Refson [29,30] to solve the corresponding equations of motion. In the simulations, we apply periodic boundary conditions, use a step size of 0.1 fs for the time integration scheme and set the fictitious mass parameter of the Nosé thermostat to a value of 100 uÅ^2. Note that we have incorporated all necessary potential model functions into our existing molecular dynamics software package TREMOLO, a load-balanced distributed memory parallel code [31]. All numerical simulations have been carried out with the TREMOLO code on the Himalaya cluster[2] at the Institute for Numerical Simulation at the University of Bonn. Further details about the algorithms and the implementation can be found in the Ref. [31,32].

Appropriate amounts of the above-mentioned species were randomly placed in a 66 Å x 66 Å x 66 Å unit cell (approximately 22500 atoms per cell) to obtain different Al-rich C-S-H gels. The NVT ensemble was first applied for 10 ps at 300 K to equilibrate the initial configuration. This equilibration period is necessary to avoid the effect of the initial random configuration. Then the temperature was increased linearly during 90 ps up to 1800 K and

---

[2] Himalaya is the high-performance cluster computer of the Institute for Numerical Simulation and the Sonderforschungsbereich 611 at the University of Bonn. Himalaya achieves 1269 GFlop/s in the Linpack benchmark test and was ranked number 428 on the June 2005 Top500 list. See also http://wissrech.ins.uni-bonn.de/research/himalaya/index.html.

maintained for 1500 ps. Although the simulation temperature may seem to be unrealistically high, it is worth noting that the thermal energy (KT) is only about 20% of the condensation energies involved in the formation of the Si-O-Si and/or Si-O-Al bonds. Thus, the employment of such a high temperature to accelerate the polymerisation process and to reduce the simulation time is well justified when studying the connectivity of the silicate chains [26]. On the other hand, the simulation time has been chosen large enough to reach convergence in the connectivity of the silicate and aluminate units. This way we ensure that the polymerisation process has been complete. Finally the temperature was decreased linearly to 300K during 500 ps, and the system was kept at this temperature throughout the last 100 ps. Note that all the values employed in this work have been averaged over the last 50 ps of the simulation.

3. Results and discussion

The discussion and presentation of our results will be made following the general Qn notation adopted from NMR experiments. Qn(mAl) denotes the connectivity of the silicate units based on the chemical shift, where n represents the number of Si-O linkages of the unit and the m index denotes how many of the involved atoms are Al (see Figure 1). The connectivity of Al atoms can also be studied in terms of an analogous $Q^{Al}n$ (mSi) notation, where n is now the number of Al-O bonds and the m index stands for the number of neighbouring Si atoms. In our molecular dynamics simulations we have determined the equilibrium percentage of the Qn(mAl) and Qn^{Al} (mSi) sites for systems which possess different Al/Si and Ca/Si ratios. In particular three different Al/Si ratios have been considered: Al/Si=0.14, Al/Si=0.20 and Al/Si=0.33. Furthermore, for each Al/Si ratio we varied the Ca/Si ratio within the range of typical cement samples (between Ca/Si= 0.95 and Ca/Si= 2.0).

First, we analysed the formation of three-dimensional networks (i.e. Q3 and Q4 sites). The existence of Q3 and Q4 units is related to the appearance of branches and rings respectively. In cement pastes the linear structures (chains) are completely dominant. However, for systems with Ca/Si ratios lower than 0.85, non-linear structures can be found as well [18, 33]. The computed %Q3+Q4 percentages are represented in Figure 2a as a function of the Ca/Si ratio for the different Al/Si ratios. Here, we display the aluminium free values (black rhombus) computed in Ref. [23]. Two main results are worth mentioning: On the one hand, it can be observed that for all analysed Al/Si systems the %Q3+Q4 percentage decreases proportionally with the Ca/Si ratio. It is remarkable that the trend predicted in Ref. [23] (black rhombus) does not change with the presence of aluminium atoms, and consequently the calcium atoms seem to equally favour the formation of linear structures. On the other hand, Figure 2a also reflects that there is a higher polymerisation degree (formation of non-linear structures) for the systems with aluminium. Therefore, the aluminium atoms favour the appearance of linkages between the chains and three-dimensional structures.

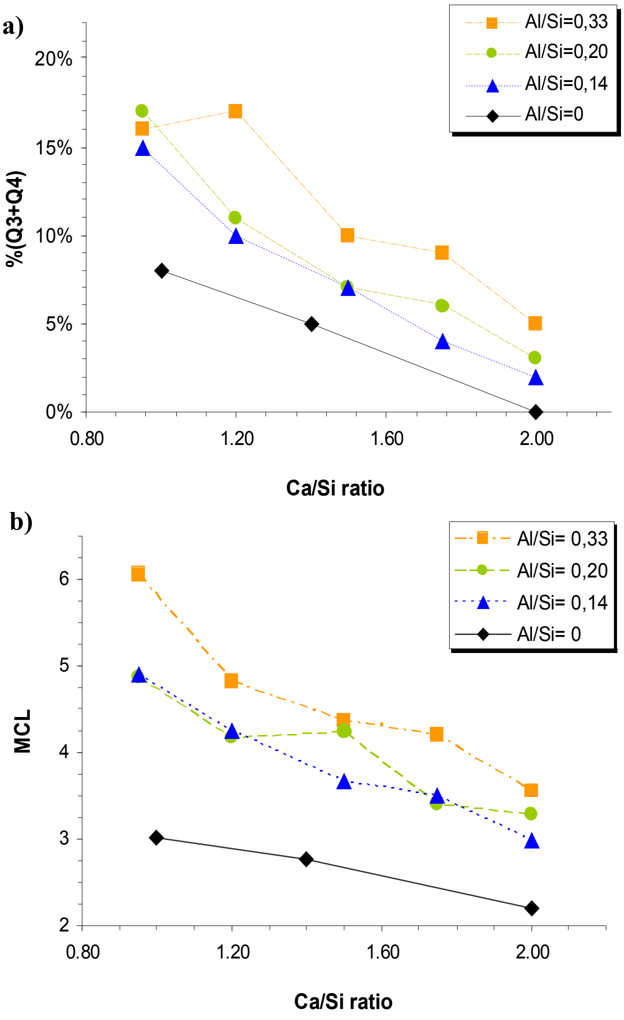

Figure 2. **a)** (Q3+Q4) sites percent represented as a function of the Ca/Si ratio for different Al/Si ratios. **b)** MCL calculated by means of equation 1 plotted versus the Ca/Si ratio for different Ca/Si ratios. In both figures the results of the previously simulations of the Al-free C-S-H gel from [23] are included.

Nevertheless, our computed %Q3+Q4 percentages are all lower than 20%, which indicates that the linear structures are still the most important features of these calcium-aluminium-silicate hydrated (C-A-S-H) systems.

Second, we analysed the linear structures in more detail. For that purpose, we calculated the main chain length (MCL) of the formed structures. The MCL can be

$$MCL = \frac{Q1 + Q2 + 3/2\ Q2(1Al)}{1/2\ Q1} \qquad (1)$$

written in terms of the Q1 and Q2 sites according to equation (1) [12]:

Figure 2b displays the mean chain length (MCL) as a function of the Ca/Si ratio for different Al/Si ratios (Al/Si=0.14, Al/Si=0.20 and Al/Si=0.33). Again, the results obtained in [23] for simulations without aluminium are also shown. First it can be seen that the MCL decreases as the Ca/Si ratio increases for all the Al/Si ratios. This tendency is in agreement with the results for systems without aluminium computed in Ref. [23] (black rhombous). However, from Figure 2b it gets clear that the MCLs increase for the system with aluminium. Moreover, the MCLs seem to be larger when the Al/Si ratio increases. This trend is in agreement with several experimental observations [10, 11, 13-16]. It is noteworthy that Richardson et al. [11] reported a MCL of 4.83 obtained by NMR analysis for C-S-H samples with a Ca/Si ratio of 1.09 and an Al/Si ratio of 0.215. Our results are in very good agreement with this value, with a MCL of 4.86 for the simulation with Ca/Si = 0.95 and Al/Si = 0.20. Note furthermore that the MCLs decrease when the calcium content is raised, following the same trend as the one found when aluminium is not incorporated in the C-S-H gel.

Third we analysed the occupancy of the aluminium atoms within the silicate chains. In Figure 3a we give the fraction of the Q1 sites with a neighbouring Al atom (i.e. the fraction %Q1(1Al)/%Q1). This value basically provides information about the amount of the terminating sites (%Q1) hosting an Al atom. As can be seen from Figure 3a, the Q1(1Al) sites represent a negligible portion of the Q1 sites (mainly Q1(0Al) sites). This is especially significant for the case of Al/Si=0.14. Consequently, our simulations are clearly in agreement with previous experimental observations [11-15] which stated that the Al atoms can hardly be accommodated at the Q1 sites.

Since the terminating sites can be discarded as likely sites for the Al atoms to enter the (alumino)silicate chains, we therefore analysed the Q2 sites. To this end, we first considered the number of Al atoms per chain occupying these Q2 sites. We give in Figure 3b the fraction $\%Q2^{Al}$(1Si) / $\%Q2^{Al}$(2Si) as a function of the Ca/Si ratio for Al/Si=0.14, Al/Si=0.2 and Al/Si=0.33. Additionally we display in Figure 3a and in Figure 3b linear fits computed by least squares linear regression. The $Q2^{Al}$(1Si) sites only appear when there are two or more Al atoms per chain, whereas the presence of $Q2^{Al}$(2Si) sites is clearly characteristic for a chain with a single Al atom. Consequently their fraction $\%Q2^{Al}$(1Si)/$\%Q2^{Al}$(2Si) provides a rough estimation of the relative amount of the chains with two Al atoms and those with just a single Al atom. As expected, our results indicate that their relative amount depends on the Al/Si ratio. For low Al/Si ratios (Al/Si=0.14) the fraction is always lower than one. This fact indicates that most of the chains contain (at most) one single Al atom per chain. For intermediate Al/Si ratios (Al/Si=0.2), the fraction is still lower than one (the linear fit is close to a value of 0.75). Thus, although the most likely case is again the one with a single Al atom per chain, the fraction of chains with two Al atoms is nevertheless a

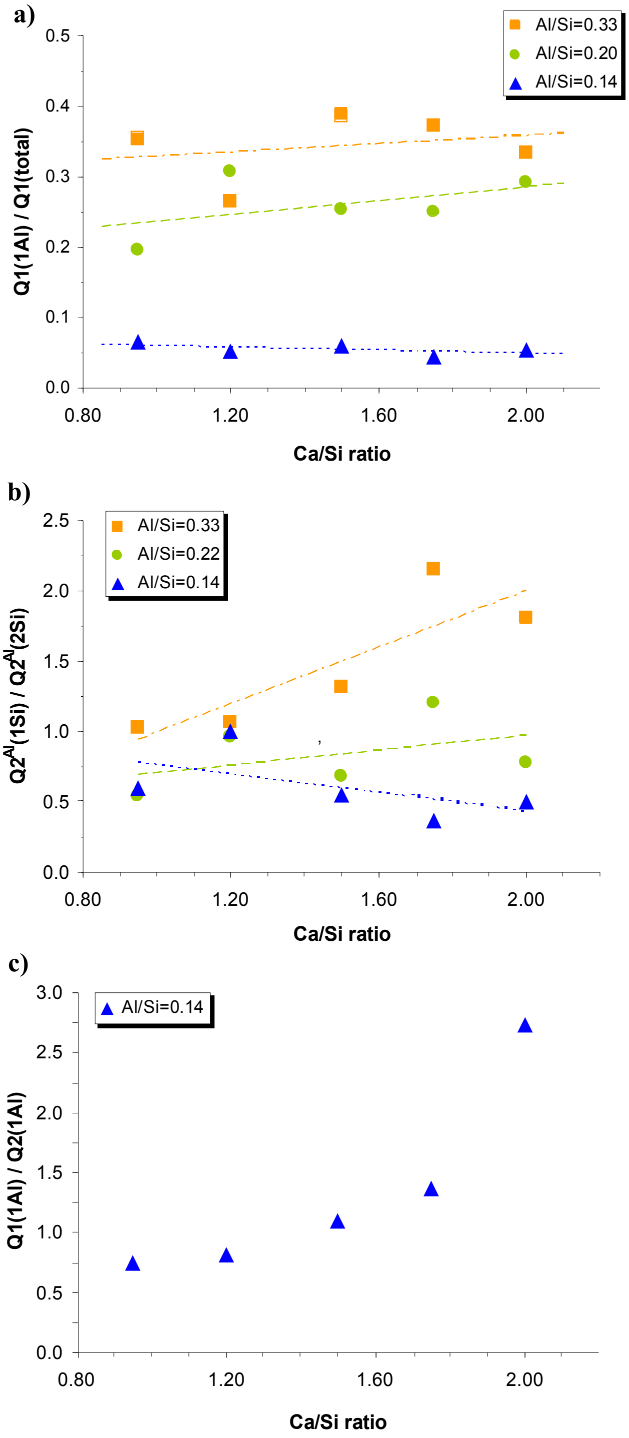

Figure 3. Graphical representation of the **a)** %Q1(1Al)/%Q1 total and **b)** $\%Q2^{Al}$ (1Si) / $\%Q2^{Al}$(2Si) relationships as function of the Ca/Si ratio for the different Al/Si ratios. The best linear fit is represented for a better view of the trend. **c)** %Q1(1Al)/ %Q2(1Al) fraction versus the Ca/Si ratio for Al/Si = 0.14 ratio.

non negligible portion of the total. However, at high Al/Si ratios (Al/Si=0.33), the fraction of $Q2^{Al}$(1Si) exceeds the fraction of $Q2^{Al}$(2Si) sites. The same is especially significant at high Ca/Si ratios. Consequently, at high Al/Si ratios our numerical simulations predict a clear predominance of chains with two Al atoms per chain. Finally, we examined the importance of the pairing sites (PS) and bridging sites (BS). As the discussion is only meaningful when there is a single Al atom per chain, we limited our analysis to the Al/Si=0.14 case. In Figure 3c we display the fraction %Q1(1Al)/%Q2(1Al) as a function of the Ca/Si ratio. We note the following: If a single Al atom is located at the pairing site (PS), there concurrently appear one Q1(1Al) site and one Q2(1Al) site, whereas if the Al atom occupies the bridging site (BS), no Q1(1Al) site appears. Our results indicate that there is a gradually raising preference of the Al atoms to go from the BSs to the PSs when the Ca/Si is raised. At low Ca/Si ratios (Ca/Si < 1.4) the Al atoms seem to prefer the BSs (Q1(1Al)/Q2(1Al) < 1), whereas at high Ca/Si ratios (Ca/Si > 1.5), the most favourable positions for the Al atoms turn to be the BSs (Q1(1Al)/Q2(1Al) >1)).

4. Conclusions The molecular dynamics method has been employed to simulate the polymerisation of aluminosilicate chains in the presence of Ca ions. The most relevant results can be summarised as follows:

First, we considered the connectivity of the aluminosilicate chains. In fact, by analysing the %Q3+Q4 sites, we have shown that the presence of Al atoms favours the formation of three-dimensional structures. Nevertheless, the still low values of the %Q3+Q4 fractions (always lower than 20%) indicate that the linear arrangements represent the most relevant features.

Second, the incorporation of Al atoms into the (alumino)silicate chains have been investigated in terms of the mean chain length (MCL). Basically our simulations showed that the presence of Al atoms entails the formation of chains with longer MCLs.

Finally, we considered the particular position of the Al atoms within the chains. By analysing the values of %Q1(1Al)/%Q1 we showed that the terminating positions seem to be unlikely sites for Al atoms. This result fairly well agrees with the existent experimental observations. Moreover we saw that, as expected, the number of Al atoms per chain depends on the Al/Si ratio. According to our molecular dynamics simulations the Al/Si=0.2 and (mainly) the Al/Si=0.33 systems contain a noticeable fraction of chains with two Al atoms. Only for the system with Al/Si=0.14 the fraction of chains with a single Al atom clearly exceeds the fraction of the chains with two Al atoms. For this last system, the occupancy of the BSs and the PSs by the Al atoms have been analysed in terms of the fraction %Q1(1Al)/%Q2(1Al). Our simulations then predict a gradual evolution from the BSs to the PSs when the Ca/Si is raised.

Acknowledgements H. Manzano acknowledges the grant received from the *EITE* association. This work has been supported by the Basque Government (NANOMATERIALES and HIBRICEM projects), the Spanish Government (project MONACEM and HIBRICAP projects), and, in parts, by the Schwerpunktprogramm 1165 and the Sonderforschungsbereich 611 of the Deutsche Forschungsgemeinschaft. We thank L. Jager and R. Wildenhues, who were involved in the development of the molecular dynamics software package TREMOLO of the Institute for Numerical Simulation.

References

[1] H. F. W. Taylor, J. Am. Ceram. Soc. **69**, 464 (1986).
[2] I. G. Richardson, Cement Concrete. Res. **34**, 1733 (2004).
[3] I. G. Richardson and G. W. Groves, Cement Concrete Res. **22**, 1001 (1992).
[4] V. S. Ramachandran and J. Beaudoin (eds.), Handbook of Analytical Techniques in Concrete Science and Technology, Building Materials Series (William Andrew Publishing/Noyes Publications, Norwich, New York, 2001).
[5] P. Colombet, A. R. Grimmer, H. Zanni and P. Sozzani (eds.), Nuclear Magnetic Resonance Spectroscopy of Cement-Based Materials (Springer, Berlin, 1998).
[6] L. S. Dent-Glasser, E. E. Lachowski, K. Mohan, and H. F. W. Taylor, Cement Concrete Res. **8**, 733 (1978).
[7] L. S. Dent-Glasser, E. E. Lachowski, M. Y. Qureshi, H. P. Calhoun, D. J. Embree, W. D. Jamieson, and C. R. Masson, Cement Concrete Res. **11**, 775 (1981).
[8] K. Mohan and H. F. W. Taylor, Cement Concrete Res. **12**, 877 (1982).
[9] S. Merlino, E. Bonaccorsi and T. Armbruster, Eur. J. Mineral. **13**, 577 (2001).
[10] E. Bonaccorsi and S. Merlino, J. Am. Ceram. Soc. **88**, 505 (2005).
[11] I. G. Richardson, A. R. Brough, R. Brydson, G. W. Groves, and C. M. Dobson, J. Am. Ceram. Soc. **76,** 2285 (1993).
[12] I. G. Richardson, Cement Concrete Res. **29**, 1131 (1999).
[13] M. D. Andersen, H. J. Jakobsen, and J. Skibsted, Inorg. Chem. **42**, 2280 (2003).
[14] M. D. Andersen, H. J. Jakobsen, and J. Skibsted, Cement Concrete Res. **43**, 587 (2004).
[15] G. K. Sun, J. F. Young and R. J. Kirkpatrick, Cement Concrete Res. **36,** 18 (2006).
[16] J. Schneider, M. A. Cincotto, H. Panepucci, Cement Concrete Res. **31**, 993 (2001).
[17] P. Faucon, A. Delagrave, J. C. Petit, C. Richet, J. M. Marchand and H. Zanni, J. Phys. Chem. B. **103**, 7796 (1999).
[18] X. Cong and R. J. Kirkpatrick, Advn. Cem. Bas. Mat. **3** 144 (1996).
[19] P. Faucon, J. M. Delaye, J. Virlet, J. F. Jacquinot and F. Adenot, Cement Concrete Res. **27**, 1581 (1997).
[20] S. A. Hamid, Z. Kristallogr. **154**, 189 (1981).
[21] S. Kashihara, S. Yamanaka, T. Inoune, T. Komatsu and H. Toyoshima. J. Am. Ceram. Soc. **11**, 3023 (1994).
[22] M. Rahman, S. Nagasahi and S. Tanaka, J. Nucl. Sci. Technol. **38**, 533 (2001).
[23] J. S. Dolado, M. Griebel, and J. Hamaekers, J. Am. Ceram. Soc. **90**, 3938 (2007).

[24] B. P. Feuston and S. H. Garofalini, Chem. Phys. Lett. **170**, 264 (1990).

[25] D. A. Litton and S. H. Garofalini. J. Appl. Phys. **89**, 6013 (2001).

[26] S. H. Zhang and S. H. Garofalini, J. Phys. Chem. B. **110**, 2233 (2006).

[27] E. B. Webb and S. H. Garofalini, Surf. Sci. **319**, 381 (1994).

[28] S. Nosé and M. L. Klein, Mol. Phys. **50**, 1055 (1983).

[29] D. Beeman, J. Comput. Phys. **20**, 130 (1976).

[30] K. Refson, Physica B. **131,** 256 (1985).

[31] M. Griebel, S. Knapek and G. Zumbusch. Numerical Simulation in Molecular Dynamics (Springer, Berlin, Heidelberg, 2007)

[32] M. Griebel and J. Hamaekers, in: Handbook of Theoretical and Computational Nanotechnology, edited by M. Rieth and W. Schommers, Vol. 9 (American Scientific Publishers, 2006) chap. 8.

[33] Y. Okada, H. Ishida, and T. Mitsuda. J. Am. Ceram. Soc. **77**, 765 (1994).